Geobiology

Geobiology (2013), **11**, 127–138 DOI: 10.1111/gbi.12023

Combining geometric morphometrics, molecular phylogeny, and micropaleontology to assess evolutionary patterns in *Mallomonas* (Synurophyceae: Heterokontophyta)

P. A. SIVER,[1] A. P. WOLFE,[2] F. J. ROHLF,[3] W. SHIN[4] AND B. Y. JO[4]

[1]*Department of Botany, Connecticut College, New London, CT, USA*
[2]*Department of Earth and Atmospheric Sciences, University of Alberta, Edmonton, AB, Canada*
[3]*Department of Ecology and Evolution, Stony Brook University, Stony Brook, NY, USA*
[4]*Department of Biology, Chungnam National University, Daejeon, Korea*

ABSTRACT

Synurophytes, also known as scaled chrysophytes, are ecologically important algae that produce an array of siliceous structures upon which their taxonomy is based. Despite occupying a key position within the photosynthetic heterokonts, the evolutionary history of synurophytes remains poorly constrained. Here, modern and Middle Eocene siliceous scales of the morphotaxon *Mallomonas insignis* are used as a model to investigate synurophyte evolutionary patterns. Structural details of scale morphology were examined comparatively with scanning electron microscopy and scored for geometric morphometric analyses to assess the stability of shape characters. Although consistent size differences exist (modern scales are larger than Eocene counterparts), the populations cannot be differentiated on the basis of shape or microstructural detail, implying considerable evolutionary stasis in scale morphology. A time-calibrated relaxed molecular clock analysis using a three-gene concatenated data set (27 strains) suggests that the *M. insignis* lineage predates the available fossil record, having diverged from closest congeneric taxa in the Cretaceous ($\geq$94 Ma). However, the molecular analysis also implies that considerable genetic variability is present within several morphotaxa of *Mallomonas*, implying that substantial genetic variability has arisen despite the retention of uniform scale morphologies, and resulting in the widespread occurrence of cryptic taxa. Results from the synurophyte lineage are consistent with the notion of protracted ghost ranges (>10 Ma) implied by the molecular phylogenies of other algal groups, together pointing to the paucity of the fossil record of these organisms on these timescales.

Received 31 May 2012; accepted 21 November 2012

Corresponding author: P. A. Siver. Tel.: +860 439 2160; fax: +860 439 2519; e-mail: pasiv@conncoll.edu

INTRODUCTION

Mallomonas Perty 1851, the most speciose genus within the class Synurophyceae (Heterokontophyta), consists of motile unicellular organisms with one or two plastids, two apically inserted flagella, and a siliceous cell covering composed of imbricated scales and bristles (Siver, 1991; Kristiansen, 2005). There are at least 172 named taxa within *Mallomonas* (Kristiansen, 2002). The genus commonly forms an important component of freshwater phytoplankton communities worldwide, particularly in oligotrophic and low alkalinity water bodies (Siver, 2003). The siliceous scales and bristles of *Mallomonas* are produced internally, each within a silica deposition vesicle, then excreted from the cell and precisely arranged around the cell membrane to form a continuous sheathing (Mignot & Brugerolle, 1982; Siver, 1991). Scales are positioned in a helical arrangement (Siver & Glew, 1990), so that each scale overlaps the scale behind it within the same row and one or more scales in the row anterior to it (Fig. 1A,B).

Synurophyte scales are flat to slightly convex plate-like structures with intricate designs that form the basis for taxonomic differentiation at the species level (Siver, 1991; Kristiansen, 2005). Although overall scale architecture remains constant within individual species, most taxa produce differentiated scales in accordance with their position

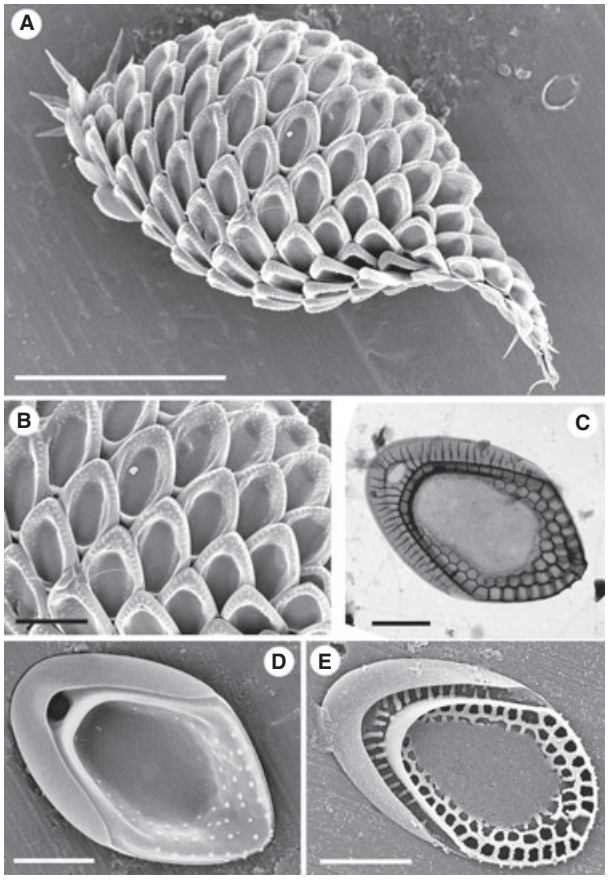

Fig. 1 Electron microscopy of *Mallomonas insignis* from modern collections. (A) Entire cell in scanning electron microscopy showing arrangement of scales in spiral rows. The posterior end of the cell is to the right. Scale bar is 20 μm. (B) Close up of the cell in (A) illustrating how each scale is overlapped by that behind it in the same spiral row and by the two in the spiral row above it. Scale bar is 5 μm. (C) Transmission electron micrographs of a typical body scale showing a series of costae radiating from the V-rib onto the posterior flange and the honeycomb structure surrounding the anterior end. Scale bar is 2 μm. (D) Body scale depicting the posterior rim, window, V-rib, and raised anterior end thinly covered by silica. Scale bar is 2 μm. (E) Body scale where the siliceous covering has dissolved, revealing the underlying structure. Scale bar is 2 μm.

on the cell. For example, specialized scales with a modified shape typically surround the flagellar pore, whereas scales with spines often adorn the posterior of the cell. The majority of the cell is covered by body scales, the most common morphology. Bristles, found on all but a few species, are elongate structures consisting of a shaft and an expanded proximal end termed the foot (Siver, 1991; Kristiansen, 2002). The foot is tucked under the distal end of a scale, and the shaft radiates from the cell.

Until recently, the fossil record of scaled chrysophytes was restricted to Late Neogene sediments, greatly limiting the appreciation of their deeper evolutionary history. Over recent years, exquisitely preserved synurophyte microfossils have been documented from Middle Eocene lake sediments in northern Canada (Siver & Wolfe, 2005a,b). In the course of these investigations, scales with pronounced morphological affinities to modern taxa have been documented, suggesting considerable evolutionary stasis with regard to synurophyte scale ultrastructure. Among these Eocene microfossils are scales that resemble those of the extant species *Mallomonas insignis* Penard. Today, *M. insignis* forms characteristic anterior and posterior spine scales, as well as unique body scales. Unlike the majority of *Mallomonas* species, *M. insignis* does not produce bristles.

Landmark-based geometric morphometric techniques are now commonly used to analyze differences in shapes of biological structures (Adams *et al.*, 2004; Zelditch *et al.*, 2004). In this approach, shape is represented by a fixed set of landmark coordinates that are standardized to eliminate the influence of differences in scale and orientation (Kendall, 1977; Zelditch *et al.*, 2004). Generalized Procrustes analysis can be used to eliminate all non-shape variations by superimposing landmark constellations for all specimens onto a mean, or consensus, constellation of landmarks. The procedure is also used to project the specimens onto a linear tangent space that provides a set of shape variables that can be used in multivariate analyses. Graphical visualizations of the results can be made using the thin-plate spline (Bookstein, 1991). For structures with a limited number of homologous landmarks, semi-landmarks can be added to capture outline shapes using an extended Procrustes superimposition procedure (Bookstein, 1997; Adams *et al.*, 2004).

Significant advances in algal molecular phylogeny include improved methodologies for the estimation of geological divergence times (Kumar, 2005; Drummond *et al.*, 2006; Drummond & Rambaut, 2007). Techniques such as relaxed molecular clocks now yield realistic timelines for phylogenetic hypotheses, yielding chronograms where branch lengths and divergence nodes are proportional to absolute time. To calibrate a phylogeny to geological time, the absolute age of one or more divergence events must be specified, most commonly from dated fossils or known geological events (Ho, 2008). Relaxed molecular clocks allow flexible rates of molecular evolution between taxa, including ancestral and descendent forms, and thus constitute a significant advance over previous models that assume constant rates of evolution for the entire tree (Thorne *et al.*, 1998; Drummond *et al.*, 2006). Chronograms based on relaxed clocks have become invaluable tools in refining our understanding of evolutionary relationships between both closely and distantly related organisms.

Since first reporting Middle Eocene *Mallomonas insignis* body scales, we have examined and measured hundreds of fossil specimens and compared these to a range of modern populations from North America, Europe, and Asia. We formalize the comparison of Eocene and modern scale morphologies using geometric morphometric analyses. We

then use time-calibrated multigene phylogenetics to estimate the age of this alga. Together, these analyses provide new insights concerning scaled chrysophyte evolution.

MATERIALS AND METHODS

Sources of *Mallomonas insignis* scales

Scales of *Mallomonas insignis* used in this study originate from ten modern and eight fossil assemblages (Table 1). Modern collections include three from North America, two from Asia, and five from Europe. Of these, three represent clones and two were from the same lake (Rökepipans Damm), but collected at different times of the year. Nine of the modern collections represent specimens from individual lakes. One modern collection, labeled 'Various lakes', represents isolated body scales from six ponds along the east coast of North America. Fossil collections originate from the post-eruptive sedimentary sequence in the Giraffe kimberlite maar in northern Canada (Siver & Wolfe, 2009). These samples comprise Middle Eocene (40–48 Ma) organic shales from depths between 97.1 m and 112.1 m in the core, where synurophyte microfossils are particularly abundant. The 18 collections were used for measurements of scale length and width and examination of ultrastructural features among anterior spine scales, body scales, and caudal spine scales. Modern sediment and Eocene mudstone samples were oxidized with a sulfuric acid–potassium dichromate solution according to Marsicano & Siver (1993), followed by repeated washes with distilled water. Aliquots of each rinsed slurry were dried onto aluminum foil, trimmed, mounted on aluminum SEM stubs using Apiezon wax, coated with a mixture of gold and palladium with a Polaron model E5 100 sputter coater, and imaged with a Leo (Zeiss) 982 field-emission scanning electron microscope (FESEM). A total of 297 body scales representing all 18 collections was used in geometric morphometric analyses (Table 1). Only specimens that were flat and not lying obliquely on the SEM stub, unobstructed, debris free, and where all landmarks could readily be identified were used in the analysis. The length and width of each body scale were measured directly from the digital image files (measurement error: ±5 nm).

Geometric morphometrics

Geometric morphometric analyses were performed using a suite of software including TpsUtility v.1.4, TpsDig v.2.05, TpsRelW v.1.42, TpsSmall v.1.2, and TpsSuper v.1.13 (Rohlf, 2007), all available from http://life.bio.sunysb.edu/morph. Forty-four landmarks were digitized from each specimen, characterizing scale perimeter outline, the V-rib, posterior rim, extent of the secondary reticulation on the scale anterior, and the 'window' on the posterior flange. Fourteen of the landmarks are fixed, and the remaining 30 represent semi-landmarks (Bookstein, 1997). The semi-landmarks are repositioned (or slid) along the outline such as to minimize Procrustes distances and to minimize any apparent shape differences due to arbitrary placement. The alignment of landmarks (Procrustes superimposition) and subsequent relative warp analysis [a principal components analysis (PCA) in linear tangent space] were performed using TpsRelW. Scale shapes plotted along the primary relative warp axes, including the consensus

Table 1 Summary and provenance of the 297 *Mallomonas insignis* body scales used in geometric morphometric analyses

Name	Sample description	Location	Number of scales	Source
Big Pond	Modern, surface sediments	North America, USA, Connecticut	10	P.A. Siver collection*
Andersen Culture	Modern, culture	North America, USA, Maine	18	R. Andersen†
Rökepipans Damm	Modern, plankton	Europe, Sweden (Oct 27, 2009)	15	G. Cronberg‡
Rökepipans Damm	Modern, plankton	Europe, Sweden (Jan 5, 2010)	18	G. Cronberg‡
Etang Cazaux	Modern, plankton	Europe, France	17	Y. Nemcova§
Etang Cazaux	Modern, surface sediments	Europe, France	21	Y. Nemcova§
Zeller Loch	Modern, plankton	Europe, Germany	17	Y. Nemcova§
Beopsu Lake	Modern, culture	Asia, Korea	19	W. Shin¶
Jeangsan Lake	Modern, culture	Asia, Korea	21	W. Shin¶
Various Lakes	Modern, surface sediments	North America, east coast sites	11	P.A. Siver collection*
GP 19-2-10	Middle Eocene, 97.1 m in core	Giraffe fossil locality	12	P.A. Siver collection*
GP 20-3-105	Middle Eocene, 100.0 m in core	Giraffe fossil locality	21	P.A. Siver collection*
GP 20-1-40	Middle Eocene, 101.7 m in core	Giraffe fossil locality	20	P.A. Siver collection*
GP 20-1-60	Middle Eocene, 101.8 m in core	Giraffe fossil locality	22	P.A. Siver collection*
GP 20-1-70	Middle Eocene, 101.9 m in core	Giraffe fossil locality	20	P.A. Siver collection*
GP 23-1-15	Middle Eocene, 109.2 m in core	Giraffe fossil locality	5	P.A. Siver collection*
GP 23-2-90	Middle Eocene, 110.8 m in core	Giraffe fossil locality	10	P.A. Siver collection*
GP 23-2-116	Middle Eocene, 112.1 m in core	Giraffe fossil locality	20	P.A. Siver collection*

*Department of Botany, Connecticut College.†Strain CCMP2549 isolated on December 1, 2003 by R. Andersen from West Harbor Pond, Maine, USA.‡Lund University, Lund, Sweden.§Y. Nemcova, Department of Botany, Charles University, Prague, Czech Republic. The plankton sample from Etang Cazaux was collected on February 2, 2010.¶Department of Biology, Chungnam National University, Daejeon, Korea.

configuration, were visualized using thin-plate spline deformation grids. The final aligned matrix of coordinates for all landmarks and semi-landmarks from each specimen was used to compute Procrustes distances (ρ) and distances in the tangent space (d). These distances were highly correlated ($r = 0.99$) justifying the use of the linear tangent space approximation for subsequent statistical analyses (Zelditch *et al.*, 2004).

Procrustes distances and Foote's index of morphological disparity (Foote, 1993; Neustupa & Nemcová, 2007) were used to investigate the degree of variation in scale shape for different sets of specimens, including the entire collection, all modern, all fossils, and each of the three clones. Procrustes distances are measured using the distances from each specimen to a reference shape (also called the consensus or mean shape). The larger the difference of an individual specimen from the consensus shape, the larger the resulting Procrustes distance. We report mean, standard deviation, minimum and maximum values of Procrustes distances obtained for each subset of specimens. Foote's index of morphological disparity, M, was measured for different groups of specimens as follows:

$$M = \sum_{i=1}^{n} (\rho^2)/(N-1)$$

where ρ = Procrustes distance for an individual scale and N is the number of scales within the population under consideration. Analysis of variance (ANOVA) was used to test for differences in Procrustes distances and scale size between fossil and modern assemblages using SPSS v.9.0.1 (SPSS Inc., Chicago, IL, USA). A general linear model multivariate analysis of variance was used to test for differences in scale shapes between fossil and modern specimens, using scores from PCA along the first two axes as dependent variables. Scheffé and Bonferroni *post hoc* tests were used to identify differences between fossil scales and distinct sets of modern assemblages, using a significance level of 0.05. Similar results were produced by both tests of significance.

Multigene phylogeny and relaxed molecular clock calculations

We used Bayesian inference under a relaxed molecular clock model derived using BEAST v.1.6.2 software (Drummond & Rambaut, 2007) to develop a phylogeny and simultaneously estimate branch divergence times for 27 strains of *Mallomonas* representing 19 species and including two strains of *M. insignis* (Table 2). A three-gene concatenated data set consisting of the 18S SSU rDNA, 28S LSU rDNA, and rbc*L* chloroplast genes was used in the analysis. Data for 19 strains (18 species) of *Mallomonas* were taken from Jo *et al.* (2011). Gene sequence data for eight additional strains, representing six species, were obtained from GenBank (two strains) or derived from new unialgal cultures (Table 2). Data derived from GenBank for *Mallomonas annulata* CCMP474 and *M. insignis*

Table 2 Strains and GenBank accession numbers for *Mallomonas* strains used in this study. Accession numbers are listed for the 18S, 28S, and rbcL genes, respectively

Species of *Mallomonas*	Strain Number	Accession Numbers
akrokomos	Posan012608J	GU935625.1; GU935647.1; GU935667.1
*alpina**	Gungnam0728071	GU935620.1; GU935642.1; GU935662.1
annulata	CCMP474	EF165127.1;EF165193.1
annulata	IIwang022407C	GU935626.1; GU935648.1; GU935668.1
areolata†	Hongseong120107D	GU935619.1; GU935641.1; GU935661.1
asmundiae‡	CCMP1658	M87333; AF409122.1; AF015585.1
bangladeshica	Hoesan061007G	GU935630.1; GU935652.1; GU935672.1
caudata	Dangge060207A	GU935629.1; GU935651.1; GU935671.1
caudata	Bangjukgo1062310A	JN991176; JN991185; JN991167
caudata§	CCMP2880	
cratis	Hoje060207B	GU935623.1; GU935645.1; GU935665.1
elongata	Mokji112407C	GU935621.1; GU935643.1; GU935663.1
heterospina	Posan012608A	GU935617.1; GU935639.1; GU935659.1
heterospina	Mulryanggji041710A	JN991179; JN991188; JN991170
insignis	Beopsu033107D	GU935634.1; GU935656.1; GU935676.1
insignis	CCMP2549	EF165118.1; EF165198.1
mangofera fo. *foveata*	Hoesan0610071	GU935633.1; GU935655.1; GU935675.1
matvienkoae	Gungnam2052507A	GU935627.1; GU935649.1; GU935669.1
matvienkoae	Mureong112807B	GU935628.1; GU935650.1; GU935670.1
matvienkoae	Mudong072410D	JN991182; JN991191; JN991173
matvienkoae	Ryujinnuma100609	JN991183; JN991192; JN991174
peronoides	Pihyangjeong092609A	JN991180; JN991189; JN991172
portae-ferreae	Dangha110407B	GU935618.1; GU935640.1; GU935660.1
pseudocratis	Seungum120107F	GU935624.1; GU935646.1; GU935666.1
punctifera	Igyo111107B	GU935632.1; GU935654.1; GU935674.1
oviformis	Wolpo112807H	GU935631.1; GU935653.1; GU935673.1
striata var. *serrata*	Hwadong103108B	GU935622.1; GU935644.1; GU935664.1

*Listed as *M. tonsurata* in GenBank.†Listed as *M. corymbosa* in GenBank.‡According to R. Andersen, these sequences were all from the same strain isolated and deposited at CCMP.§In the CCMP collection as *M. ovalis*.

CCMP 2549 were contributed by R.A. Andersen (National Center for Marine Algae and Microbiota, Bigelow Laboratory for Ocean Sciences, East Bothbay, Maine, USA). The six unialgal cultures were established by isolating cells from small ponds in Korea and maintained using DYIII medium (Lehman, 1976) buffered to pH 7.0 with 2-(N-morpholino) ethanesulfonic acid (MES). The methodology of Jo *et al.* (2011) was used to extract, amplify, and sequence the three genes from all six cultures. The combined data set yielded two strains each of *M. insignis*, *M. heterospina,* and *M. annulata*, three of *M. caudata*, and four of *M. matvienkoae*. Gene sequences were aligned using Mafft v.6.864 (Katoh & Toh, 2008), and the final concatenated file was created using Phyutility v.2.2.4 (Smith & Dunn, 2008).

The uncorrelated lognormal model was used to estimate rate variation across all branches. Age estimates for fossil calibrations were treated as probabilistic priors, rather than point estimates (Ho & Phillips, 2009). We attached lognormal priors for the split between *Mallomonas asmundiae* and *M. striata* and for the split between *M. matvienkoae* and *M. caudata*. In both cases, we used an offset of 40 Ma, a mean of 0.5, and a standard deviation of 1.0. Scales of *M. asmundiae* are well represented in sediments from the Giraffe locality (Siver *et al.*, 2009), estimated to have a minimum age of approximately 40 Ma (Siver & Wolfe, 2009; Doria *et al.*, 2011). In addition, this deposit has yielded numerous scales that correspond to *M. matvienkoae*. A generalized time reversible (GTR) + Γ site model was applied to the three-gene concatenated data set, and a uniform Yule tree prior was used to model speciation. The analysis was run for 10 million generations with the chain sampled every 1000 generations. The initial 2500 trees (2.5 million generations) were removed as burn-in and the remaining 7500 trees used to construct the final chronogram. The final consensus tree, along with both posterior probabilities and age estimates for all branches, was visualized using FigTree v.1.3.1 (http://tree.bio.ed.ac.uk/software/figtree/).

RESULTS

A species concept for modern *Mallomonas insignis*

Cells are ellipsoidal to ovoid with a tapering tail and covered with three types of scales: anterior spined scales, body scales, and posterior spined scales (Fig. 1A). Cells vary greatly in size with most between 45 and 80 μm in length and 22 and 35 μm in width, and the posterior tail is often twisted or curved. The anterior portion of the cell consists of one or two whorls of overlapping spine-bearing scales surrounding the flagellar pore, positioned such that spines protrude at approximately 45° angles relative to the longitudinal axis of the cell. Collectively, anterior spined scales form the crown of the cell. Body scales are arranged in spiral rows, with each row originating with an anterior spined scale and terminating at the posterior tail. The longitudinal axis of body scales is approximately perpendicular to the longitudinal axis of the cell. Each scale within a spiral row is partially overlapped by the scale positioned behind it in the same row and by two scales in the spiral row above it (Fig. 1B).

Body scales are oval, with a posterior rim that encircles approximately 50% of the scale perimeter and extends over most of the posterior flange, a V-rib with branches that terminate near the scale margin above the ends of the posterior rim, and a prominent raised portion that encircles the entire anterior end (Figs 1C,D and 2). Body scales from modern specimens range in size from 5.2 to 8.4 μm in length and 2.8 and 5.2 μm in width (Table 3). The base of the V-rib is broadly rounded, often U-shaped, and development of the V-rib hood ranges from slight (Fig. 2C,E) to extensive (Fig. 2F). Each scale consists of a base plate, two series of ribs, and a thin surface covering (Figs 1C–E and 2). The base plate consists of very small and irregularly spaced pores. A series of parallel and evenly spaced ribs originates at the V-rib, radiates onto the posterior flange, and terminates under the posterior rim

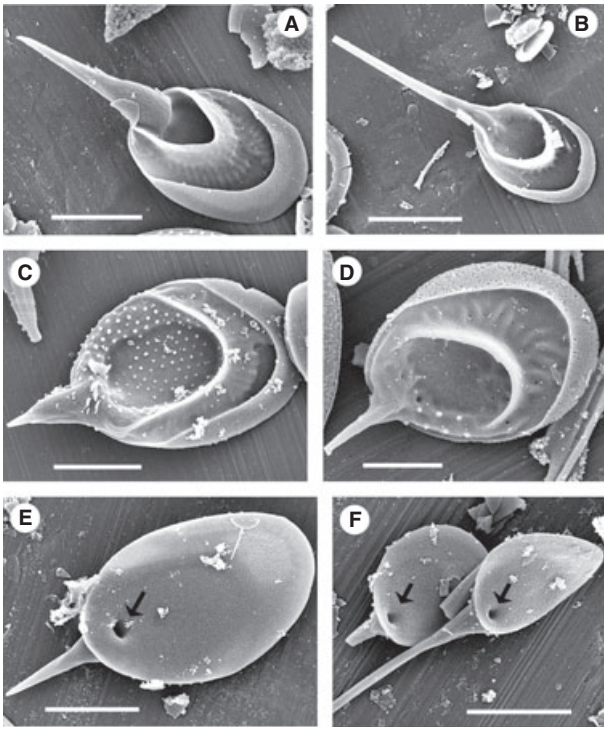

Fig. 2 Scanning electron micrographs of spined scale type in modern *Mallomonas insignis* specimens. (A, C and E) Anterior spined scales. (B, D and F) Caudal spined scales. Arrows in (E and F) indicate the large pore at the base of the spine on the underside of the scale. Scale bars are 2 μm except for (E) where scale bar 1 μm.

Table 3 Mean and standard deviation (SD) of the length and width of body scales from modern, fossil, and summed body scales of *Mallomonas insignis*

	Length (μm)		Width (μm)		
Type	SD	Mean	Mean	SD	*n*
Modern	7.0	0.66	4.3	0.50	158
Fossil	5.8	0.45	3.8	0.25	139
All scales	6.4	0.81	4.1	0.48	297

(Fig. 1C,E). Ribs are reduced or lacking on the posterior flange immediately behind the base of the V-rib, forming a distinctive space called the window (Figs 1C,D and 2). Another series of secondary ribs form a honeycomb pattern that encircles the anterior margin and extends to varying degrees down along the inside arms of the V-rib to the base of the V-rib (Fig. 1C, D, E). The shield is devoid of secondary ribs. On complete scales, a thin layer of silica covers the anterior honeycomb rib system, the shield, and the posterior flange (Fig. 2). Small papillae are present on the surface of the scale, most notably on the anterior raised region and occasionally on the shield.

Anterior spine scales have the same basic morphology as body scales, but with less pronounced features (Fig. 3A,C, E). The V-rib is often reduced, asymmetric, and situated in a more anterior position, yielding a more extensive posterior flange (Fig. 3A). Secondary rib patterns are also less developed, yielding a smaller raised anterior region and a less pronounced window on the flange. Spines are hollow and taper from a wide base to a pointed or bifurcating tip and are often lined with ridges. Spines range in length from 0.5 to 5.0 μm, and each terminates as a large pore along the underside of the scale (Fig. 3E).

Caudal spine scales are reduced in size, often only 2–3 μm in diameter, more circular in outline, and with reduced secondary features (Fig. 3B,D,F). The V-rib is less distinct, often becoming a circular rib extending from the base of the spine. The rib system, characteristic of body scales, is highly reduced or altogether lacking on caudal scales. Spines are often long relative to the diameter of the scale, but slender compared to those on anterior scales.

Morphological comparisons between modern and Eocene scales

The investigated samples from the Giraffe Eocene material all contain *Mallomonas insignis* scales referrable to the three scale types that comprise whole cells in modern counterpart populations. All morphological features found on modern scales occur in fossil specimens (Fig. 4), and

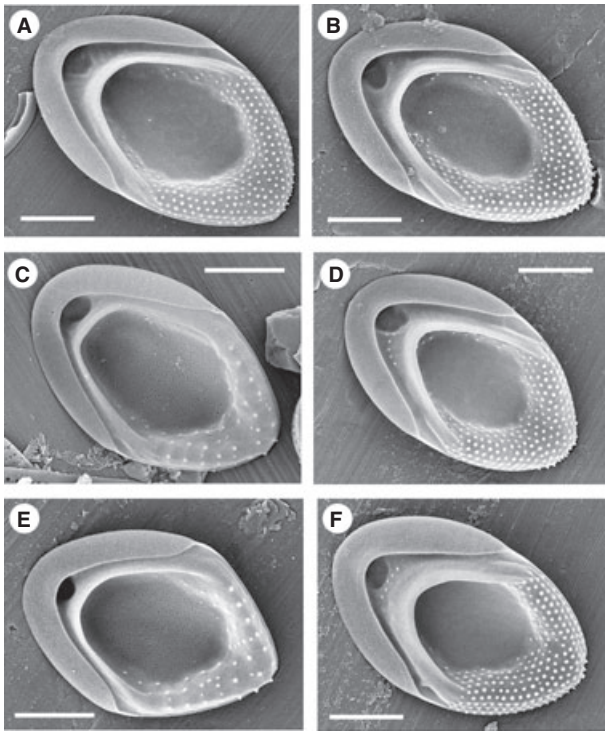

Fig. 3 Scanning electron micrographs depicting the range of body scales found on modern *Mallomonas insignis* specimens. Note the shape of the scale perimeter, V-rib, window, and the distribution of surface papillae. Scales are from Rökepipans Damm, Sweden (A, B), Big Pond, Connecticut, USA. (C, D), and Etang Cazaux, France (E, F). Scale bars are 2 μm.

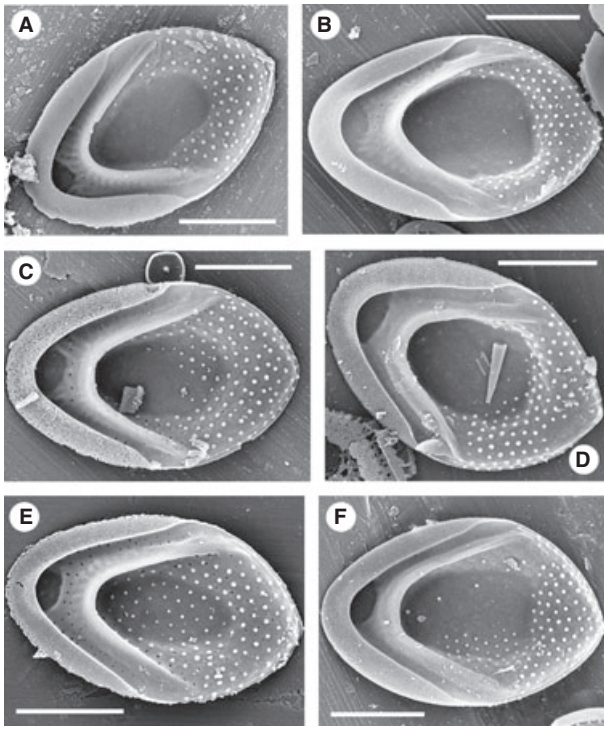

Fig. 4 Scanning electron micrographs depicting the range of body scales in Eocene *Mallomonas insignis* specimens from the Giraffe locality. Note the shape of the scale perimeter, V-rib, window, and the distribution of surface papillae. Scale bars are 2 μm.

no single character can consistently separate Eocene from modern populations. On a purely qualitative basis, a larger proportion of modern scales have U-shaped V-ribs, but the complete spectrum of V-rib morphology in modern scales is also present in Eocene scales. The tips of spines on caudal scales are splayed on a few, but not all, fossil specimens, a feature that was not observed on any modern specimen. Both modern and fossil scales have small papillae covering most of the surface of the raised anterior portion, sometimes extending onto the shield. Despite an overarching ultrastructural similarity, modern body scales of *Mallomonas insignis* are significantly larger than Eocene specimens (Table 3). On average, modern scales were 1.2 μm longer and 0.5 μm wider than fossil scales, with only minimal overlap between the two groups (Fig. 5).

Geometric morphometric analysis

Geometric morphometrics enable the formalization of shape variations between modern and fossil body scales. The distribution of fossil scale shapes along the first two axes of the relative warp analysis is largely contained within the shape space represented by all modern specimens used in this study (Fig. 6A). These two axes accounted for 80.4% of total shape variation. Although not shown here, significant overlap in shape between modern and fossil specimens was also present along axis 3. In general, the width and extent of the posterior rim around the scale perimeter, and the size and shape of the posterior window, are remarkably constant over the two-dimensional shape space depicted in Fig. 6B. However, along axis 1, scales become slightly elongate (higher length/width ratios) with a more extensive secondary layer that extends farther down along the V-rib, and have a broader V-rib base (Fig. 6B, compare thin-plate splines 1, 4, and 7 with 3, 6, and 9). In contrast, along axis 2, scales become progressively more oval in outline (decreasing length/width ratios), with a wider and more extensive shield. Nevertheless, the point of intersection between the secondary layer and the V-rib remains similar along axis 2. Scale length and width are positively correlated with axis 1, whereas width is negatively correlated with axis 2.

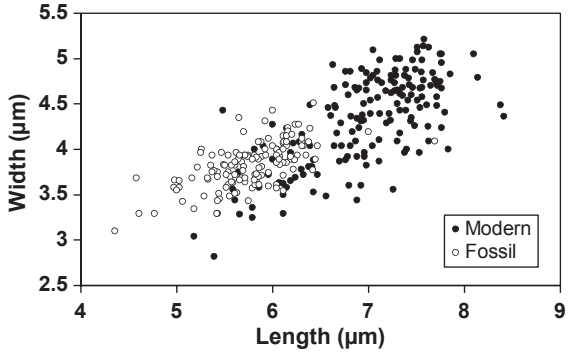

Fig. 5 Relationship between the length and width of body scales in Eocene (open circles) and modern (solid circles) specimens of *Mallomonas insignis*.

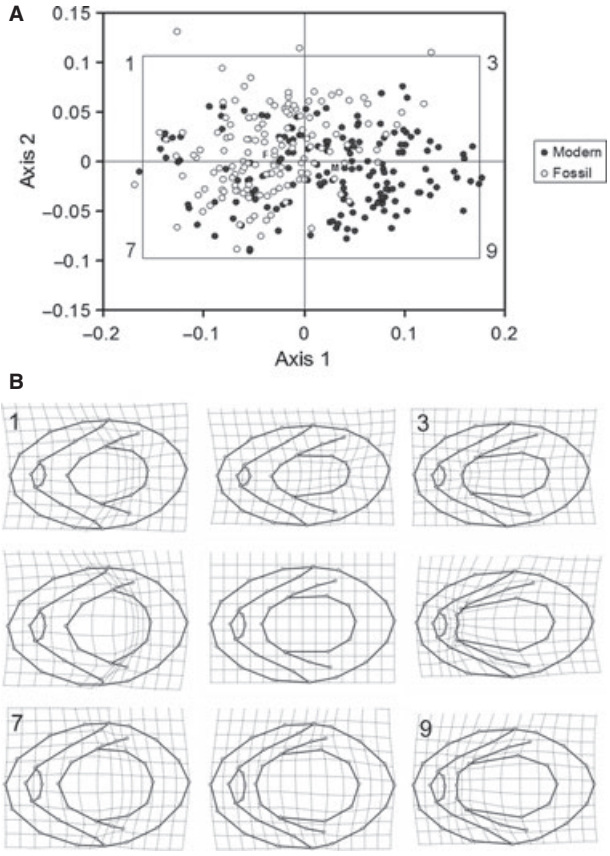

Fig. 6 Shape analysis of *Mallomonas insignis* scales. Relative warp analysis (A) and grid line deformation plots (B) for modern and fossil scales of *Mallomonas insignis*. Mean scores for fossil and modern scales are depicted on the relative warp plot by an F and M, respectively. The first two axes accounted for 80.4% of the total shape variation. The nine deformation plots correspond to the positions at the corners (marked 1, 3, 7, and 9) of the inner box and where the box crosses the axes.

Most of the shape variation in a sample of modern scales can be captured in a two-dimensional space. Some of the modern scales are slightly more elongate with a broader V-rib base and a more extensive secondary layer as compared to Eocene fossils. Collectively, these features resulted in a slight, but significant, shift in mean shape between fossil and modern scales along both relative warp axes 1 and 2 captured by the position of their respective centroids (Figs 6A and 7). No differences were found along axis 3. Despite these differences, shapes of fossil scales are not significantly different from individual populations including those from France and Sweden, Big Pond in Connecticut, and the collection of lakes from eastern North America. Along axis 1 only, fossil scales are significantly different from those from the Asian lakes, Zeller Loch, and the iso-

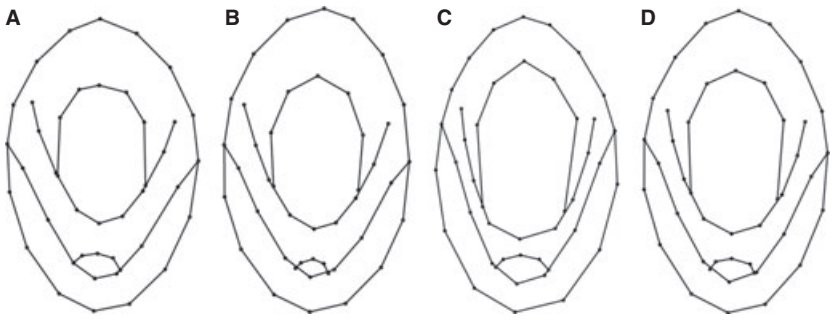

Fig. 7 Consensus line plots for *Mallomonas insignis* scales. Results are shown for (A) all fossil specimens; (B) two populations from Rökepipans Damm, Sweden; (C) the culture isolate from Maine, USA; and (D) all modern scales.

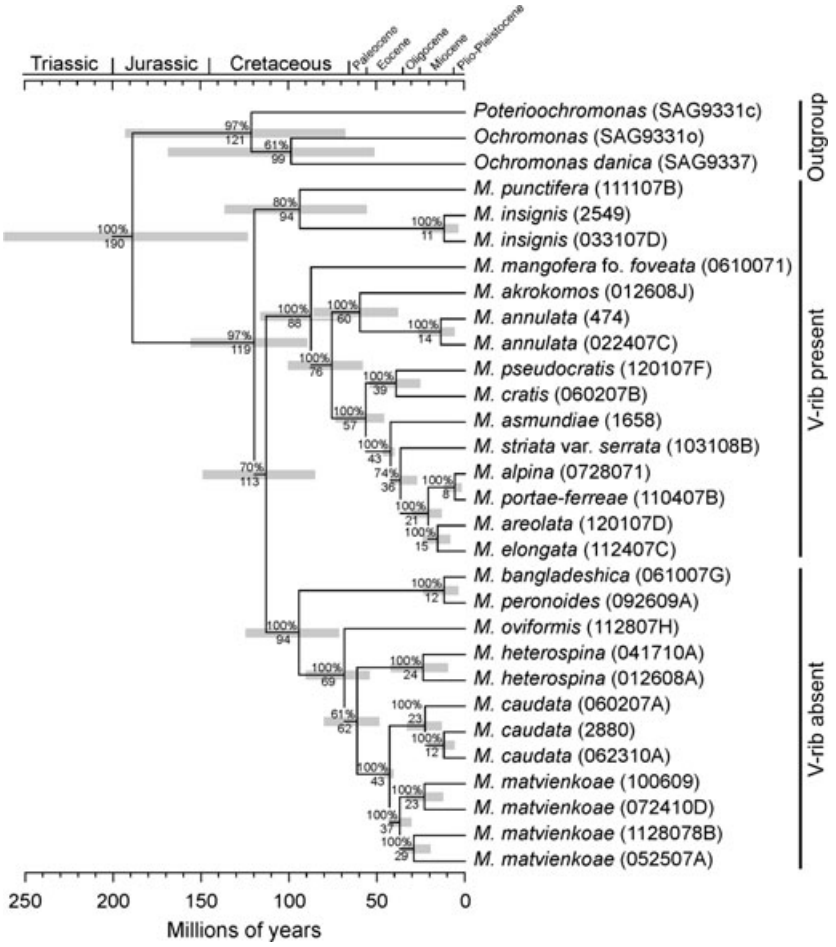

Fig. 8 Time-calibrated phylogenetic tree for 29 *Mallomonas* taxa based on the concatenated 18s rDNA, 28s rDNA, and rbcL data set, calibrated at two nodes using microfossils from the Giraffe locality. The first number at each node represents the mean divergence time (in Ma), and the second is posterior probability. Open bars represent 95% highest posterior densities for each node age.

late from Maine (Fig. 7C). It is worth noting that no significant differences were found between any of the eight fossil assemblages representing different sections of the Giraffe core.

The extent of variation in scale shape was further analyzed using Procrustes distances and Foote's index of morphological disparity (Table 4). Differences in mean Procrustes distances for all of the 18 groups of specimens examined are small, ranging from 0.09 to 0.14. There are no significant differences in the mean Procrustes distance between modern, fossil, culture isolate (clones from Beopsu, Jeangsan and Maine) or total scale populations (Table 4). Similarly, differences in Foote's index of morphological disparity are minimal for all sets of specimens.

Table 4 Mean, standard deviation (SD), minimum and maximum Procrustes distances and Foote's index of morphological disparity, for all scales, modern scales, scales only from clones, and fossil scales

Category	Procrustes distance				Foote's disparity
	Mean	Minimum	Maximum	SD	
All specimens (n = 297)	0.11	0.05	0.21	0.03	0.013
All modern (n = 159)	0.12	0.05	0.20	0.03	0.014
Modern clones (n = 58)	0.12	0.07	0.18	0.02	0.015
Fossils (n = 139)	0.11	0.06	0.21	0.03	0.012

Summarily, the most consistent difference between modern and Eocene scales of *M. insignis* is that relating to overall scale size (Table 3, Fig. 5).

Relaxed molecular clock phylogenetic analysis

Based on the three-gene concatenated alignment, species of *Mallomonas* with scales lacking a V-rib form a well-supported monophyletic clade that diverged from V-ribbed taxa approximately 113 Ma (Fig. 8). Estimated divergence times followed by posterior probabilities are shown for each node, with 95% highest posterior density intervals for divergence times represented by horizontal bars. The clade containing *Mallomonas insignis* and *M. punctifera* diverged from all other species within the genus at 119 Ma, while *M. bangladeshica* diverged at the base of the clade containing taxa lacking a V-rib at 94 Ma. The five species of *Mallomonas* represented by multiple strains were all monophyletic with well-supported posterior probabilities (100%). This observation supports the leading role of morphology in scaled chrysophyte taxonomy (Siver, 1991; Kristiansen, 2005). At the same time, strains representing the same morphotaxa express considerable intraclade genetic variability, with divergence times ranging from 11 to 37 Ma for strains of *M. insignis* and *M. matvienkoae*, respectively. Therefore, considerable potential exists for the evolution of cryptic taxa within the mallomonadacean scaled chrysophytes, as intimated by previous results (Boo *et al.*, 2010).

DISCUSSION

Based on detailed ultrastructural and shape analyses, scales representing modern populations of *Mallomonas insignis* from different continents all share characteristics expressed by specimens recovered from the Middle Eocene Giraffe locality. The considerable ultrastructural complexity of each of the three scale types found on *M. insignis* cells proved similar for fossil and modern specimens, and no character unique to either group could be identified. Total variation in body scale shape and architecture from the Giraffe locality, as determined using geometric morphometric analyses, is largely constrained by that represented by modern counterparts. As a result, from a strictly morphological perspective, fossil scales from the Giraffe material can be classified taxonomically as *M. insignis*, with the implication that this taxon is relatively ancient, having survived largely unchanged for at least 40 Ma. Clearly, scales of intermediate age would be desirable in these analyses. However, despite considerable searches spanning a range of Paleogene and Neogene lacustrine shales, we have yet to identify such specimens.

Despite ultrastructural similarities and overlapping scale shapes, some differences exist between fossil and modern body scales, however subtle. Importantly, modern scales are significantly larger than fossil counterparts, being about 20% longer and 10% wider. In addition, modern scales have a broader range in shape, more frequently exhibiting a broader, more U-shaped, V-rib, and an anterior secondary layer extending farther down the V-rib. The wider range in scale shape in modern specimens likely results from evolutionary changes since the Eocene, perhaps including allopatric processes given that the modern specimens considered originate from three continents.

The degree of evolutionary stasis suggested by the conservative nature of *M. insignis* morphology has been advanced for other species of scaled chrysophytes present in the Giraffe core, including *Synura recurvata* (similar to the modern taxon *Synura uvella*; Siver & Wolfe, 2005b), *Mallomonas bangledeshica* (Siver & Wolfe, 2009), and *Mallomonas asmundiae* (Siver *et al.*, 2009). Unlike these previous reports, the current analysis of *M. insignis* includes examination of multiple scale types found on the cell and a refined quantitative analysis of scale morphology. Evolutionary stasis within algae preserved in sediments from the Giraffe locality is not restricted to scaled chrysophytes, given similar results for diatom taxa including *Aulacoseira* (Wolfe *et al.*, 2006), *Eunotia* (Siver & Wolfe, 2007), *Discotella*, *Punctastriata*, and *Cyclotella* (Wolfe & Siver, 2009) and *Pinnularia* (Souffreau *et al.*, 2011).

How evolutionary stasis is maintained in protists such as scaled chrysophytes and diatoms is not known, but it likely relates to advantages conferred by traits of scale or frustule morphology coupled to the reproductive strategies of the organism in question. The exact evolutionary advantages conferred by the intricate details of siliceous structures in scaled chrysophytes (Siver, 2003) and diatoms (Round *et al.*, 1990; Sims *et al.*, 2006) remain unclear. What is becoming evident, however, is that these lineages have existed over tens of millions of years without substantial modification of many diagnostic morphological characters (Siver & Wolfe, 2005a; Sims *et al.*, 2006; Harwood *et al.*, 2007; Parfrey *et al.*, 2011). In the case of *Mallomonas insignis*, the structure and detail of all three scale types, along with the shape of the body scales, have remained largely unchanged since at least the Eocene, with the exception of an enlargement of mean scale size. However, the intricate architecture of scale arrangement in *Mallomonas* had fully evolved by the Middle Eocene (Siver & Wolfe, 2010).

We hypothesize that evolutionary stasis of siliceous structures is, in part, the result of long-term maintenance of a stable genotype propagated through predominately asexual reproduction, coupled with the dispersal of genetically similar cysts over broad geographic ranges. Both asexual and sexual reproduction in chrysophytes result in the formation of a vase-shaped siliceous structure, the cyst, which serves as a resting stage for the organism and the seed source for future populations (Cronberg, 1986; Sandgren, 1988, 1991). Although sexual reproduction has been observed in a few loricate genera (Kristiansen, 2005) and in cultures of *Dinobryon* (Sandgren, 1981) and *Synura* (Sandgren & Flanagan, 1986), this process is rarely observed in field collections and almost never in *Mallomonas*. Exceptionally, Wawrik (1960) and Kristiansen (1961) observed cells of *M. caudata* align and fuse tail to tail, eventually forming a cyst. If such a process was common, fused cells should have one half of their scales whorled in the opposite direction to the other half, and to our knowledge, such remains have never been reported. What is commonly observed in *Mallomonas* are single cells forming endogenous cysts as the result of asexual reproduction. Formation and subsequent germination of asexually formed cysts has the net effect of perpetuating genetic stability. There is emerging support for this type of stability among heterokont algae. For example, genetic structure in the diatom *Skeletonema marinoi* inferred from strains resurrected from sediments spanning approximately 100 years and over 40,000 generations has remained remarkably stable (Härnström *et al.*, 2011). In this case, microsatellite markers demonstrate that the endemic character of a local population has been maintained despite continuous exchange with water masses harboring genetically distinct strains of *S. marinoi* and that highly conservative genotypes are fostered by combinations of high growth rates, dense cell concentrations, short generation times, and predominately asexual modes of reproduction. At present, we are unable to falsify the possibility of analogous processes in scaled chrysophytes and indeed of their perpetuation over significantly longer timescales.

However, not all scaled chrysophytes present in the Giraffe material display the same degree of apparent evolutionary stasis identified in *M. insignis*. Instead, three general categories are represented. The first includes taxa such as *M. insignis* having scale types that are not readily distinguished from modern forms and conferring a high degree of evolutionary stasis. The second includes scale types that differ somewhat from modern counterparts but can nonetheless be aligned with modern species flocks (Siver & Wolfe, 2005b). A third group includes forms that are believed to be extinct (Siver & Wolfe, 2010). Taken together, these observations suggest that the evolutionary history of scaled chrysophytes is characterized by marked differences in rates of morphological divergence between taxa and that selective gradients do not influence all scaled chrysophytes in a uniform way, despite overarching similarities in the autecologies of co-occurrent species.

The presence of anterior spine scales, coupled with the lack of bristles, makes *M. insignis* unique within *Mallomonas*. In addition, unlike most congeneric species, spines of *M. insignis* scales are hollow with a large pore opening on the underside of the base plate, in this way more similar to spines in the related genus *Synura*. Initial multigene molecular clock analyses suggest that the split between *Mallomonas* and *Synura* is ancient, potentially in the approximately 300 Ma range (Boo *et al.*, 2010). In the subsequent phylogenetic analysis of Jo *et al.* (2011), two robust clades of *Mallomonas* were identified, one characterized by scales lacking a V-rib, with *M. bangladeshica* at the base, and a second consisting of all species possessing a V-rib or homologous structure, with *M. insignis* and *M. punctifera* at the base. Our present results similarly divide taxa with and without a V-rib (Fig. 8) and further indicate that the divergence of these two clades occurred early in the evolution of *Mallomonas*.

The unique suite of morphological characters present in *M. insignis*, coupled with its early divergence, suggests that it represents an ancient lineage within *Mallomonas* and that evolutionary stasis in scale morphology may be considerably older than the 40 Ma milepost provided by the Giraffe material. Indeed, the relaxed molecular clock results suggest that *M. insignis* and *M. punctifera* diverged from other congeners in the Early Cretaceous. What then becomes intriguing is that the two strains of *M. insignis* used in our molecular analysis are estimated to have diverged from each other approximately 11 Ma ago. The antiquity of these modern strains provides independent support for the hypothesis of protracted evolutionary stasis with respect to scale morphology, but simultaneously demonstrates that uniform scale morphology can mask considerable genetic variability. Cryptic speciation, in which genetic diversity is masked by a common ultrastructure, has been recognized in other scaled chrysophytes including the cosmopolitan organism *Synura petersenii* (Kynclova *et al.*, 2010). In such cases, traditional species concepts are supplanted by complexes for which differences in morphology are subtle or non-existent, but for which considerable genetic divergence is evident. It is noteworthy that *S. petersenii* is also an early-divergent scaled chrysophyte, based on time-calibrated molecular clock estimates (Boo *et al.*, 2010). Given the early divergence of *M. insignis* implied by our analysis (Fig. 8), coupled with its widespread distribution (Kristiansen, 2002), more in-depth analyses of genetic variability in this taxon are likely to provide further insights on questions pertaining to the evolution and biogeography of the scaled chrysophyte lineage.

We recognize that molecular chronograms based on few calibration points can be problematic and should be viewed

with caution (Hug & Roger, 2007; Weir & Schluter, 2008). It is thus not surprising that the range of posterior age produced by our phylogenetic model is large, especially for more ancient nodes (Fig. 8). However, we emphasize that, at present, the Giraffe fossil locality is the only known deposit containing unambiguous scaled chrysophytes of Paleogene age. We anticipate that the future will yield additional microfossils with which to calibrate our preliminary topology, ultimately reducing uncertainty concerning the timing of key evolutionary events in scaled chrysophytes.

CONCLUSIONS

Although the understanding of synurophyte evolution is still in its infancy, what is gradually emerging from combined interrogations of fossil and molecular data is a picture whereby these organisms are considerably older than previously assumed and furthermore characterized by ghost lineages that encapsulate tens of millions of years. Because similar results have been obtained from freshwater diatoms (Souffreau *et al.*, 2011), the evolutionary trajectories of non-marine ochrophytes as a whole are progressively becoming closer in line with other unicellular algal photoautotrophs (Falkowski *et al.*, 2004), with the prediction that their originations are ultimately much older than currently revealed by the fossil record. In this regard, the judicious combination of morphological, molecular, and micropaleontological approaches represents an approach having considerable potential to further refine evolutionary hypotheses concerning the history of these ecologically important organisms.

ACKNOWLEDGMENTS

We thank Anne-Marie Lott for assembling information for this project, Jeremy Beaulieu for assistance in running BEAST, Yvonne Nemcová for imaging specimens from French and German lakes, Gertrud Cronberg for providing samples from Sweden, and Robert Andersen for providing the *Mallomonas insignis* culture from Maine. This work was funded with support to PAS from the National Science Foundation (DEB-0716606, DEB-1049583, and DEB-1144098) and to APW by the Natural Sciences and Engineering Research Council of Canada.

REFERENCES

Adams DC, Rohlf FJ, Slice DE (2004) Geometric morphometrics: ten years of progress following the 'revolution'. *The Italian Journal of Zoology* **71**, 5–16.

Boo SM, Kim HS, Shin W, Boo GH, Cho SM, Jo BY, Kim J-H, Kim JH, Yang EC, Siver PA, Wolfe AP, Bhattacharya D, Andersen RA, Yoon HS (2010) Complex phylogeographic patterns in the freshwater alga *Synura* provide new insights into ubiquity vs. endemism in microbial eukaryotes. *Molecular Ecology* **19**, 4328–4338.

Bookstein FL (1991) *Morphological Tools for Landmark Data: Geometry and Biology*, Cambridge University Press, Cambridge, UK.

Bookstein FL (1997) Landmark methods for forms without landmarks: morphometrics of group differences in outline shape. *Medical Image Analysis* **1**, 225–243.

Cronberg G (1986) Chrysophycean cysts and scales in lake sediments. In *Chrysophytes: Aspects and Problems* (eds Kristiansen J, Andersen RA). Cambridge University Press, New York, pp. 281–315.

Doria G, Royer DL, Wolfe AP, Fox A, Westgate JA, Beerling DJ (2011) Declining atmospheric CO_2 during the late Middle Eocene climate transition. *American Journal Science* **311**, 63–75.

Drummond AJ, Rambaut A (2007) BEAST: Bayesian evolutionary analysis by sampling trees. *BMC Evolutionary Biology* **7**, 214–221.

Drummond AJ, HO SYW, Phillips MJ, Rambaut A (2006) Relaxed phylogenetics and dating with confidence. *PLoS Biology* **4**, 699–710.

Falkowski PG, Katz ME, Knoll AH, Quigg A, Raven JA, Schofield O, Taylor FJR (2004) The evolution of modern eukaryotic phytoplankton. *Science* **305**, 354–360.

Foote M (1993) Contributions of individual taxa to overall morphological disparity. *Paleobiology* **19**, 403–419.

Härnström K, Ellegaard M, Andersen T, Godhe A (2011) Hundred years of genetic structure in a sediment revived diatom population. *Proceedings of the National Academy Sciences* **108**, 4252–4257.

Harwood DM, Nikolaev VA, Winter DM (2007) Cretaceous records of diatom evolution, radiation, and expansion. In *From Pond Scum to Carbon Sink: Geological and Environmental Applications of the Diatoms* (ed. Starratt S), Paleontological Society Papers **13**, pp. 33–59.

Ho S (2008) The molecular clock and estimating species divergence. *Nature Education* **1**, 1–3.

Ho S, Phillips MJ (2009) Accounting for calibration uncertainty in phylogenetic estimation of evolutionary divergence times. *Systematic Biology* **58**, 367–380.

Hug LA, Roger AJ (2007) The impact of fossils and taxon sampling on ancient molecular dating analyses. *Molecular Biology and Evolution* **24**, 1889–1897.

Jo BY, Shin W, Boo SM, Kim HS, Siver PA (2011) Studies on ultrastructure and three-gene phylogeny of the genus *Mallomonas* (Synurophyceae). *Journal of Phycology* **47**, 415–425.

Katoh K, Toh H (2008) Recent developments in the MAFFT multiple sequence alignment program. *Briefings in Bioinformatics* **9**, 286–298.

Kendall D (1977) The diffusion of shape. *Advances in Applied Probability* **9**, 428–430.

Kristiansen J (1961) Sexual reproduction in *Mallomonas caudata*. *Botanisk Tidsskrift* **57**, 306–309.

Kristiansen J (2002) The genus *Mallomonas* (Synurophyceae): a taxonomic survey based on the ultrastructure of silica scales and bristles. *Opera Botanica* **139**, 1–218.

Kristiansen J (2005) *Golden Algae – A Biology of Chrysophytes*, Gantner Verlag, Koenigstein, Germany.

Kumar S (2005) Molecular clocks: four decades of evolution. *Nature Reviews Genetics* **6**, 654–662.

Kynclova A, Skaloud P, Skaloudova M (2010) Unveiling hidden diversity in the *Synura petersenii* species complex (Synurophyceae, Heterokontophyta). *Nova Hedwigia Beiheft* **136**, 283–298.

Lehman JT (1976) Ecological and nutritional studies on *Dinobryon* Ehrenb.: seasonal periodicity and the phosphate toxicity problem. *Limnology and Oceanography* **21**, 646–658.

Marsicano LJ, Siver PA (1993) A paleolimnological assessment of lake acidification in five Connecticut lakes. *Journal of Paleolimnology* **9**, 209–221.

Mignot JP, Brugerolle G (1982) Scale formation in chrysomonad flagellates. *Journal of Ultrastructure Research* **81**, 13–26.

Neustupa J, Nemcová Y (2007) A geometric morphometric study of the variation in scales of *Mallomonas striata* (Synurophyceae, Heterokontophyta). *Phycologia* **46**, 123–130.

Parfrey LW, Lahr DJG, Knoll AH, Katz LA (2011) Estimating the timing of early eukaryotic diversification with multigene molecular clocks. *Proceedings of the National Academy Sciences* **108**, 13624–13629.

Rohlf FJ (2007) *TPS Series*. Department Ecology & Evolution, SUNY-Stony Brook, NY.

Round FE, Crawford RM, Mann DG (1990) *The Diatoms: Biology and Morphology of the Genera*, Cambridge University Press, Cambridge, UK.

Sandgren CD (1988) The ecology of chrysophyte flagellates: their growth and perennation strategies as freshwater phytoplankton. In *Growth and Reproductive Strategies of Freshwater Phytoplankton* (ed. Sandgren CD), Cambridge University Press, Cambridge, UK, pp. 9–104.

Sandgren CD (1991) Chrysophyte reproduction and resting cysts: a paleolimnologist's primer. *Journal of Paleolimnology* **5**, 1–9.

Sandgren CD, Flanagan J (1986) Heterothallic sexuality and density dependent encystment in the chrysophycean alga *Synura petersenii* Korsh. *Journal of Phycology* **22**, 206–216.

Sims PA, Mann DG, Medlin LK (2006) Evolution of the diatoms: insights from fossil, biological and molecular data. *Phycologia* **45**, 361–402.

Siver PA (1991) *The Biology of Mallomonas: Morphology, Taxonomy and Ecology*, Kluwer Academic Publishers, Dordrecht, the Netherlands.

Siver PA (2003) The Synurophyceae. In *Freshwater algae of North America* (eds Wehr J, Sheath RG) Academic Press, San Francisco, CA, USA, pp. 523–558.

Siver PA, Glew JR (1990) The arrangement of scales and bristles on *Mallomonas*: a proposed mechanism for the formation of the cell covering. *Canadian Journal of Botany* **68**, 374–380.

Siver PA, Wolfe AP (2005a) Eocene scaled chrysophytes with pronounced modern affinities. *International Journal of Plant Science* **166**, 533–536.

Siver PA, Wolfe AP (2005b) Scaled chrysophytes in Middle Eocene lake sediments from northwestern Canada, including descriptions of six new species. *Nova Hedwigia Beiheft* **136**, 295–308.

Siver PA, Wolfe AP (2007) *Eunotia* spp. (Bacillariophyceae) from Middle Eocene lake sediments and comments on the origin of the diatom raphe. *Canadian Journal of Botany* **85**, 83–90.

Siver PA, Wolfe AP (2009) Tropical ochrophyte algae from the Eocene of northern Canada: a biogeographic response to past global warming. *Palaios* **24**, 192–198.

Siver PA, Wolfe AP (2010) A whole-cell reconstruction of *Mallomonas porifera* Siver and Wolfe from the Eocene: implications for the evolution of chrysophyte cell architecture. *Nova Hedwigia Beiheft* **136**, 117–127.

Siver PA, Lott AM, Wolfe AP (2009) Taxonomic significance of asymmetrical helmet and lance bristles in the genus *Mallomonas* and their discovery in Eocene lake sediments. *European Journal of Phycology* **44**, 447–460.

Smith SA, Dunn CW (2008) Phyutility: a phyloinformatics tool for trees, alignments and molecular data. *Bioinformatics* **24**, 715–716.

Souffreau C, Verbruggen H, Wolfe AP, Vanormelingen P, Siver PA, Cox J, Mann DG, Van de Vijver B, Sabbe K, Vyverman W (2011) A time-calibrated multi-gene phylogeny of the diatom genus *Pinnularia*. *Molecular Phylogenetics and Evolution* **61**, 866–879.

Thorne JL, Kishino H, Painter IS (1998) Estimating the rate of evolution of the rate of molecular evolution. *Molecular Biology and Evolution* **15**, 1647–1657.

Wawrik F (1960) Sexualität bei *Mallomonas fastigata* var. *kriegerii*. *Archiv für Protistenkunde* **104**, 541–544.

Weir JT, Schluter D (2008) Calibrating the avian molecular clock. *Molecular Ecology* **17**, 2321–2328.

Wolfe AP, Siver PA (2009) Three extant genera of freshwater Thalassiosiroid diatoms from middle Eocene sediments in northern Canada. *American Journal of Botany* **96**, 487–497.

Wolfe AP, Edlund MB, Sweet AR, Creighton S (2006) A first account of organelle preservation in Eocene nonmarine diatoms: observations and paleobiological implications. *Palaios* **21**, 298–304.

Zelditch MI, Swiderski DL, Sheets DH, Fink WL (2004) *Geometric Morphometrics for Biologists: A Primer*, Elsevier Academic Press, London.